Enhanced Natural Killer Cell Binding and Activation by Low-Fucose IgG1 Antibody Results in Potent Antibody-Dependent Cellular Cytotoxicity Induction at Lower Antigen Density

Rinpei Niwa,[1] Mikiko Sakurada,[1] Yukari Kobayashi,[1] Aya Uehara,[1] Kouji Matsushima,[2] Ryuzo Ueda,[3] Kazuyasu Nakamura,[1] and Kenya Shitara[1]

[1]Tokyo Research Laboratories, Kyowa Hakko Kogyo, Co., Ltd.; [2]Department of Molecular Preventive Medicine, School of Medicine, University of Tokyo, Tokyo, Japan; and [3]Department of Internal Medicine and Molecular Science, Nagoya City University Graduate School of Medical Science, Nagoya, Japan

ABSTRACT

Purpose: **Recent studies have revealed that fucose removal from the oligosaccharides of human IgG1 antibodies results in a significant enhancement of antibody-dependent cellular cytotoxicity (ADCC) via improved IgG1 binding to FcγRIIIa. In this report, we investigated the relationship between enhanced ADCC and antigen density on target cells using IgG1 antibodies with reduced fucose.**

Experimental Design: **Using EL4 cell-derived transfectants with differential expression levels of exogenous human CC chemokine receptor 4 or human CD20 as target cells, ADCC of fucose variants of chimeric IgG1 antibodies specific for these antigens were measured. We further investigated IgG1 binding to natural killer (NK) cells and NK cell activation during ADCC induction to elucidate the mechanism by which low-fucose IgG1 induces ADCC upon target cells with low antigen expression.**

Results: **Low-fucose IgG1s showed potent ADCC at low antigen densities at which their corresponding high-fucose counterparts could not induce measurable ADCC. The quantitative analysis revealed that fucose depletion could reduce the antigen amount on target cells required for constant degrees of ADCC induction by 10-fold for CC chemokine receptor 4 and 3-fold for CD20. IgG1 binding to NK cells was increased by ligating IgG1 with clustered antigen, especially for low-fucose IgG1. Up-regulation of an activation marker, CD69, on NK cells, particularly the $CD56^{dim}$ subset, in the presence of both the antibody and target cells was much greater for the low-fucose antibodies.**

Conclusions: **Our data showed that fucose removal from IgG1 could reduce the antigen amount required for ADCC induction via efficient recruitment and activation of NK cells.**

Received 11/5/04; revised 12/21/04; accepted 12/29/04.
The costs of publication of this article were defrayed in part by the payment of page charges. This article must therefore be hereby marked *advertisement* in accordance with 18 U.S.C. Section 1734 solely to indicate this fact.

Requests for reprints: Kenya Shitara, Division of Immunology, Tokyo Research Laboratories, Kyowa Hakko Kogyo, Co., Ltd., 3-6-6 Asahi-machi, Machida-shi, Tokyo 194-8533, Japan. Phone: 81-42-725-0857; Fax: 81-42-725-2689; E-mail: kshitara@kyowa.co.jp.

INTRODUCTION

Antibodies of the human IgG1 isotype are commonly used for therapeutic applications as they can mediate multiple effector functions including antibody-dependent cellular cytotoxicity (ADCC), complement-dependent cytotoxicity (CDC), and direct apoptosis induction (1–3). ADCC, a lytic attack on antibody-targeted cells, is triggered following binding of leukocyte receptors (FcγR) to the antibody Fc region. Several mouse and clinical studies indicate that ADCC is an important therapeutic mechanism of clinically effective antibodies (4–7). FcγRIIIa is the predominant FcγR of natural killer (NK) cells responsible for ADCC activation. The FcγRIIIa gene (*FCGR3A*) displays an allelic polymorphism that generates receptors containing either a phenylalanine (F) or a valine (V) at a position critical in mediating ADCC, amino acid position 158. This variation results in human IgG1 antibodies binding with higher affinity to the NK cells of homozygous *FCGR3A*-158V donors than those of homozygous *FCGR3A*-158F donors, and seems to result in more effective NK cell activation (8, 9). Importantly, several reports have recently shown that *FCGR3A* genotype influences the clinical efficacy of human IgG1-type anti-CD20 antibody rituximab (3, 10, 11) with the clinical response of patients bearing FcγRIIIa-158F being significantly inferior to the patients with the FcγRIIIa-158V receptors (5–7). These reports underscore the importance of ADCC in clinical outcomes.

ADCC activity is influenced by the structure of complex-type oligosaccharides linked to CH2 domain of the antibody Fc region. The content of galactose (12, 13), bisecting *N*-acetylglucosamine (14, 15), and fucose (16, 17) in the antibody oligosaccharide have each been reported to effect ADCC. In previous studies, we have shown that fucose is the most critical antibody oligosaccharide component and that the removal of fucose from IgG1 oligosaccharides results in a very significant enhancement of both ADCC *in vitro* (~100 fold) and antitumor activity *in vivo* (17, 18). However, many therapeutic antibodies currently approved or under clinical development are produced using Chinese hamster ovary cells that express high level of α1,6-fucosyltransferase and consequently produce low amounts antibody lacking fucose (17). Therefore, we generated a fucosyltransferase knockout Chinese hamster ovary cell line that can stably produce nonfucosylated antibodies with enhanced ADCC (19) that behaves in other respects indistinguishable from the parental line.

Although therapeutic antibodies are demonstrating increasing success in the clinic, especially in the field of cancer treatment (1, 2), the full potential may be limited by the low and

variable antigen expression on the target cells. This is due to three factors that can limit the efficacy of therapeutic antibodies. First, there are often individual patients or clinical subtypes of the cancer that are unresponsive to the antibody therapy due to limited or heterogeneous antigen expression (3, 20). Second, residual tumor cells after antibody therapy may be selected to express less antigen than pretreated tumor cells (21, 22), become resistant to additional treatment, and, thus, may lead to poor prognosis. Third, antigen may be thought unsuitable as antibody targets due to low antigen expression. Consequently, it is important to improve antibody efficacy for tumor cells with lower antigen expression level.

Previous studies have shown that ADCC depends on antigen expression levels on target cells (23). Hence, we asked if low-fucose IgG1 with enhanced ADCC might overcome the problem of low antigen density on target cells. In this study, we quantitatively analyzed the effect of antigen levels on the ability of low-fucose IgG1 to induce ADCC on target cells to determine the potential therapeutic advantage of low-fucose IgG1 for future clinical applications. Additionally, we focused on NK cell binding to low-fucose IgG1 and the resultant cellular activation to understand the mechanism of potent ADCC induction, especially at low antigen density.

MATERIALS AND METHODS

Blood Donors. Blood donors were randomly selected from healthy volunteers registered at Tokyo Research Laboratories, Kyowa Hakko Kogyo, Co., Ltd. All donors gave written informed consent before analyses.

Cell Lines. Mouse T-cell lymphoma cell line EL4, human B lymphoma cell line CA46, CCRF-SB (ATCC CCL-120), ST486, Raji, and Daudi were purchased from the American Type Culture Collection (Rockville, MD). A human B lymphoma cell line P32/ISH (JCRB0095) was purchased from Health Science Research Resources Bank (Osaka, Japan).

Preparation of Target Cell Lines. A human CC chemokine receptor 4 (CCR4) expression plasmid CAG-pcDNA-CCR4 bas been previously described (18). An expression plasmid encoding human CD20, designated pKANTEXCD20, was constructed by inserting *CD20* gene, cloned from a human leukocyte cDNA library (BD Biosciences Clontech, Palo Alto, CA) by PCR into mammalian cell expression vector pKANTEX93 (24). EL4 cells were transfected with CAG-pcDNA-CCR4 or pKANTEXCD20 by electroporation and grown in the presence of 0.5 mg/mL G418 sulfate to obtain G418-resistant clones. For some clones with higher CD20 expression, gene amplification in the presence of methotorexate (4-amino-10-methylpteroylglutamic acid, MTX) was done. Multiple clones with differential protein expression levels were screened by nonquantative flow cytometry as described below.

Antigen Expression Analysis by Flow Cytometry. A nonquantitative flow cytometry was done for the screening of transfected target cell clones. Biotinylated KM2760 was prepared using EZ-Link Sulfo-NHS-LC-Biotin (Pierce, Rockford, IL) as described by the manufacturer. Approximately 1×10^6 cells were stained for 1 hour on ice with 3 μg/mL of biotin-labeled KM2760 for $CCR4^+$ clones or a 10-fold dilution of FITC-conjugated anti-CD20 monoclonal antibody (Beckman Coulter, Tokyo, Japan) for $CD20^+$ clones. For CCR4-expressing clones, cells were washed and then stained with phycoerythrin-conjugated streptavidin (Becton Dickinson Japan, Tokyo, Japan) as the secondary reagent. The stained cells were analyzed on an EPICS XL-MCL flow cytometer (Beckman Coulter).

To determine the absolute number of the antibody binding sites per cell, a quantitative flow cytometry analysis (25) was done using DAKO QIFIKIT (DakoCytomation, Kyoto, Japan). Briefly, 1×10^6 cells were stained for 1 hour on ice with saturating concentration of KM2160 (60 μg/mL) for $CCR4^+$ clones or mouse anti-CD20 monoclonal antibody (clone 2H7, BD Biosciences PharMingen, San Diego, CA; 40 μg/mL) for $CD20^+$ clones. Cells were then washed and then stained with FITC-conjugated anti-mouse IgG (DakoCytomation) for 1 hour on ice. Standard beads coated with known amount of mouse IgG molecules were also stained with FITC-conjugated anti-mouse IgG. The stained samples were analyzed using a flow cytometer, and the numbers of binding sites per cell were calculated by comparing the mean fluorescent intensity value of the stained cells to a standard curve obtained by regression analysis of the mean fluorescent intensity values of standard beads.

Cytotoxicity Assay. ADCC was measured using a standard 4-hour ^{51}Cr release assay as previously described (17). CDC was measured by a nonradioactive method. Target cells (1×10^6 cells/50 μL medium), varying concentrations of antibodies (in 50 μL medium), and human complement serum (50 μL, ×2 diluted with medium; Sigma, St. Louis, MO) were distributed into 96-well flat-bottomed plates. All cells and reagents were diluted with RPMI 1640 (Life Technologies, New York, NY) containing 10% heat-inactivated fetal bovine serum. After incubation at 37°C for 2 hours, aliquots of the cell proliferation reagent WST-1 (Roche Diagnostic GmbH, Penzberg, Germany) were added to each well (15 μL) and the plates were incubated for a further 4 hours to allow the formazan dye production by the metabolically active cells. The percent cytotoxicity was calculated from the absorbance at 450 nm minus the reference absorbance at 650 nm ($A_{450} - A_{650}$) of each well according to the formula:

$$\% \text{ cytotoxicity} = 100 \times (E - S)/(M - S)$$

where E is the $A_{450} - A_{650}$ of experimental well, S is that in the absence of monoclonal antibody (cells were incubated with medium and complement alone), and M is that of medium and complement alone.

Isolation of Natural Killer Cells. Peripheral blood mononuclear cells (PBMC) were prepared from peripheral blood by density gradient centrifugation using Lymphoprep (AXIS SHIELD, Dundee, United Kingdom). PBMC were then subjected to negative magnetic sorting to obtain NK cell fraction, by removing CD3, CD14, CD19, CD36, and IgE-positive cells using MACS NK cell isolation kit and MidiMACS (Miltenyi Biotec, Bergisch Gladbach, Germany). The phenotype of the isolated NK cell fraction was confirmed as >95% $CD56^+CD3^-$ before any experiments.

IgG1 Binding Analysis to Natural Killer Cells. Isolated NK cells (1×10^6) were incubated on ice for 1 hour with 1% bovine serum albumin (BSA)/PBS containing 10 μg/mL IgG1. After incubation with IgG1, cells were washed twice with PBS

and analyzed after staining with phycoerythrin-conjugated anti-human IgG Fab'$_2$ (DakoCytomation) on a flow cytometer. In some experiments, IgG1 was incubated with 20 μg/mL BSA-conjugated CCR4 peptide before the incubation with NK cells for the IgG1 ligation. The BSA-conjugated CCR4 peptide was prepared by conjugating the partial CCR4 peptide including the binding site of KM2760 and KM3060 (corresponding to amino acid residues 2 to 29 of human CCR4; ref. 18) to the amino groups of BSA using 4-(*N*-maleimidomethyl)-cyclohexane-1-carboxylate *N*-hydroxysuccinimido ester (Sigma) as previously described (26).

Analysis of Natural Killer Cell Activation. Isolated NK cells (1×10^5/100 μL medium/well) and the equal number of target cells in 100 μL medium were dispensed in round-bottom 96-well plate. IgG1 (final concentration, 1 μg/mL) or medium alone were added to each well and incubated at 37°C. Cells were harvested periodically (4, 24, and 72 hours) and double-stained with phycoerythrin-conjugated anti-CD56 monoclonal antibody (Beckman Coulter) and FITC-conjugated anti-CD69 monoclonal antibody (BD Biosciences PharMingen) on ice for 1 hour. After washing, NK cells, which can be gated out by their relative smaller values of forward scatter and side scatter compared with target cells, were measured of their CD56/CD69 expression on a flow cytometer.

RESULTS

Antibody-Dependent Cellular Cytotoxicity of Anti-CD20 IgG1 Fucose Variants against B Lymphoma Cell Lines with Differential CD20 Expression Levels. KM3065 (17) is a low-fucose variant of anti-CD20 chimeric IgG1 rituximab, which is widely used for the treatment of B-cell disorders. KM3065 and rituximab have identical amino acid sequences and thus show identical CD20 binding activities, whereas they differ in the percentage of antibody lacking fucose-containing carbohydrates linked to Asn^{297} in CH2 domain of heavy chain (Table 1). Due to its low fucose contents and consequent strong FcγRIIIa binding, KM3065 has been shown to exhibit enhanced ADCC against CD20$^+$ Raji cells and WIL2-S cells (17, 27). However, how the ADCC enhancement by defucosylation was influenced by the intrinsic properties of target cells remains to be verified. To investigate the relationships between the enhancement of ADCC by defucosylation and the antigen expression level on target cells, we investigated ADCC of the two anti-CD20 IgG1s upon six B lymphoma cell lines with differential CD20 expression levels as shown in Fig. 1. CD20 binding sites on each cell lines were determined by quantitative flow cytometry method (25) with values ranging within an order of magnitude (7.8×10^4 to 5.9×10^5). Using human PBMCs with effector cells, KM3065 showed enhanced ADCC upon all the target cell lines compared with rituximab. Although the correlation between the ADCC and the numbers of CD20 binding sites was not statistically significant, ADCC values mediated by both the two IgG1s tended to be higher for target cell lines with higher CD20 expression. The result suggests that target cell lines from different origins are not suitable for the quantitative analysis of ADCC depending on antigen expression because their own

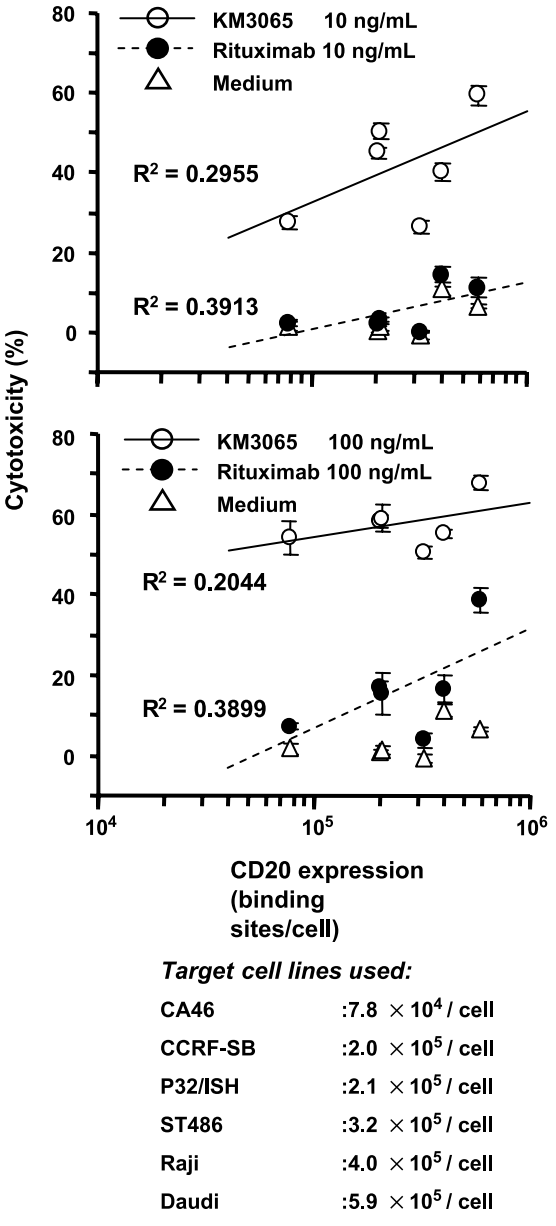

Fig. 1 ADCC of anti-CD20 chimeric IgG1s against B lymphoma cell lines with differential CD20 expression. The cytotoxicities in the presence of 10 ng/mL (*top*) or 100 ng/mL (*bottom*) of anti-CD20 IgG1s against six B lymphoma cell lines determined by 4-hour ^{51}Cr release assays are shown. PBMC from a healthy blood donor were used as effector cells, with an effector-to target ratio of 25:1. *Y*-axis, cytotoxicity (%), mean ± SD (n = 3). *X*-axis, number of CD20 binding sites per cell on each target cell line. The target cell lines used and the corresponding numbers of CD20 binding sites were also shown.

Table 1 Content of nonfucosylated N-linked oligosaccharide in each IgG1 compositions

IgG1	Specificity	%Fucose(−)	Reference
KM2760	Human CCR4	93	Niwa et al. (18)
KM3060	Human CCR4	9	Niwa et al. (18)
KM3065	Human CD20	91	Shinkawa et al. (17)
Rituximab	Human CD20	6	Shinkawa et al. (17)

cellular backgrounds, other than the antigen amount, determines their inherent sensitivities against ADCC.

Preparation of Transfectant Target Cells with Varying Expression Levels of Exogenous Antigen. To establish a simpler system for the investigation of the influence of the antigen amount on tumor cells independently from different cellular backgrounds, we next constructed panels of transfectant tumor cell lines with wide ranges of antigen expression levels. We used two antigen-specific systems for this aim, CCR4 and CD20. In addition to anti-CD20 IgG1s described above, two fucose variants of chimeric anti-CCR4 IgG1s have also been generated: the conventional highly fucosylated anti-CCR4 IgG1, KM3060, and its low-fucose counterpart, KM2760 (Table 1). They share identical amino acid sequences and CCR4 binding activities, whereas KM2760 has shown enhanced ADCC against $CCR4^+$ T leukemia cells (18).

Panels of target cells with a range of expression levels of the chosen antigens were constructed by transfecting *CCR4* or *CD20* genes into murine thymoma EL4 cells. EL4 cells were chosen as the host cell to generate target cells for the quantitative evaluation of ADCC because of their resistance to antibody-independent cytotoxic activity of human NK cells that could obscure antibody-dependent cytotoxicity. Following single cell cloning, eight CCR4-positive clones (designated CCR4/EL4-A to CCR4/EL4-H) and seven CD20-positive clones (CD20/EL4-A to CD20/EL4-G) were screened by nonquantitative flow cytometry as illustrated in Fig. 2. To generate high expressing $CD20^+$ clones, gene amplification in the presence of MTX was used: CD20/EL4-D and CD20/EL4-F were produced using 200 nmol/L MTX selection and CD20/EL4-G was produced using 1,000 nmol/L MTX.

The numbers of antibody binding sites per cell on each established EL4 clones were then determined using quantitative flow cytometry method and ranged from 1.3×10^3 to 5.4×10^4 for CCR4 and from 1.2×10^4 to 5.8×10^5 for CD20 (Table 2). All clones were confirmed to have similar cell diameters by flow cytometry (data not shown), implying that antigen densities on the surface of each target cell were expected to be proportional to the numbers of antibody binding sites shown in Table 2. Although the parent murine EL4 cell would not be expected to express human antigens and no visible staining were observed in nonquantitative flow cytometry (Fig. 2), the methodology used calculated ~600 sites per cell for each of the antigens. This was probably because of the marginal nonspecific or cross-reactive staining in the quantitative flow cytometry analysis. It should be noted that the CCR4 expression levels of all the human T-cell leukemia cell lines that we have previously described (18) ranged between those of CCR4/EL4 clone A and clone G used in these studies, as observed in nonquantitative flow cytometry (data not shown). CD20 expression on clinical B lymphoma cells has been reported to be $\sim 10^5$, although it depends on the clinical subtype of the lymphoma to some extent (3, 28–30). Taken together, the expression levels of the target cell clones established in this study were considered to be representative of the *in vivo* expression levels of patient's tumor cells.

Antibody-Dependent Cellular Cytotoxicity of IgG1 Fucose Variants against Experimental Target Cells with Various Antigen Expression Levels. We next measured the ADCC of both IgG1 fucose variants upon the experimental target cell lines described above. As shown in Fig. 3, using PBMC from peripheral blood of two healthy donors (donor A and B) as effector cells, the low-fucose KM2760 showed higher ADCC activity than that of the high-fucose KM3060 against each of the CCR4-transfected target cells. Analysis of the ADCC activity of the two IgG1s were each found to fit to a sigmoid-shaped curve with different maximal levels of cytotoxicity for

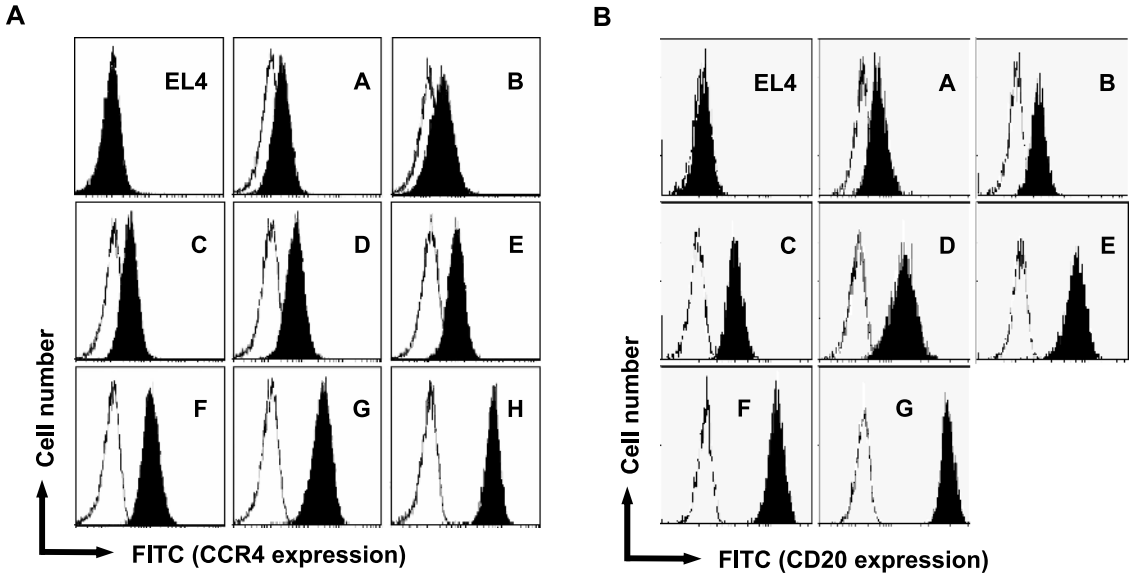

Fig. 2 Relative antigen expression levels in the established target cell clones. The parental EL4 cells and the clones with various expression levels of exogenous human *CCR4* (*A*) or *CD20* (*B*) genes were stained with biotynylated KM2760 or FITC-conjugated anti-CD20 monoclonal antibody, respectively. For CCR4-expressing clones, cells were washed and then stained with avidin-conjugated FITC as the secondary reagent. The stained cells (*filled histograms*) and the reference unstained samples (*blank histograms*) were then analyzed by flow cytometry. Clone names are indicated in each panel: A to H in *A*, clone CCR4/EL4-A to CCR4/EL4-H; A to G in *B*, clone CD20/EL4-A to CD20/EL4-G.

Table 2 Numbers of binding sites on the established target cell clones

CCR4-positive clones		CD20-positive clones	
Clone	Binding sites*	Clone	Binding sites†
CCR4/EL4-A	1.3×10^3	CD20/EL4-A	1.2×10^4
CCR4/EL4-B	1.6×10^3	CD20/EL4-B	1.5×10^4
CCR4/EL4-C	2.6×10^3	CD20/EL4-C	2.5×10^4
CCR4/EL4-D	4.6×10^3	CD20/EL4-D	4.1×10^4
CCR4/EL4-E	5.8×10^3	CD20/EL4-E	6.7×10^4
CCR4/EL4-F	1.5×10^4	CD20/EL4-F	2.1×10^5
CCR4/EL4-G	1.7×10^4	CD20/EL4-G	5.8×10^5
CCR4/EL4-H	5.4×10^4		
EL4	6.6×10^2	EL4	6.1×10^2

*Number of CCR4 binding sites per cell determined by quantitative flow cytometry.

†Number of CD20 binding sites per cell determined by quantitative flow cytometry.

the different IgG1s calculated by the four-parameter regression equations (Table 3). In addition, the minimum amount of antigen that was required to induce detectable level of ADCC of KM2760 was less than that of KM3060. For example, with donor A effector cells, KM2760 exhibited ADCC against all CCR4-expressing clones ($\geq 1.3 \times 10^3$ CCR4 binding sites), whereas KM3060 required at least 1.5×10^4 CCR4 binding sites in the presence of 3 μg/mL IgG1s (Fig. 3, *top right*). Further, we calculated the number of CCR4 binding sites required to achieve the half-maximal cytotoxicitiy of KM3060 for both KM2760 and KM3060 (Table 3). For example, with PBMC from donor A and 3 μg/mL antibody concentration, KM3060 required 2.1×10^4 CCR4 binding sites on target cells for its half-maximal cytotoxicity (14.4%), whereas KM2760 required only 9.6-fold less antigen to achieve the same level of cytotoxicity, indicating KM2760 required only approximately one tenth of CCR4 expression than KM3060 in this experimental condition. Similar quantitative relationships in the ADCC of the two IgG1s were observed in all cases in Fig. 3 except for a little smaller difference in efficacies of the two IgG1s (5.6-fold) with donor A PBMC and 0.1 μg/mL antibody concentration.

A similar advantage of low-fucose IgG1 in the lysis of low-antigen-expressing cells and the maximal cytotoxicity was also observed for CD20 system using PBMC from two other donors (Fig. 4), indicating that low-fucose IgG1 can reduce the antigen number required for ADCC in CD20 system in addition to increasing the maximal ADCC achievable. However, the shifts in required antigen amount was somewhat less compared with CCR4 system (the low-fucose KM3065 required ~3-fold less CD20 amount than rituximab in each experimental condition; Table 4). This may be due to the relatively higher ADCC mediated by the high-fucose IgG1 (rituximab). We also investigated another important Fc-mediated function of antibody, CDC, of the two anti-CD20 IgG1s on the CD20-transferred target clones (Fig. 5). In contrast to ADCC, the cytotoxicities of the two IgG1s were not significantly different. The anti-CCR4 IgG1s did not exhibit any measurable CDC activity against any of the CCR4-transfected target cells irrespective of their fucose contents (data not shown). These differing results between CCR4 and CD20 might be due to many factors including the expression levels of the antigens, the inherent capacity of the antigens to mediate CDC, or the antigen-binding affinity of individual antibody clone.

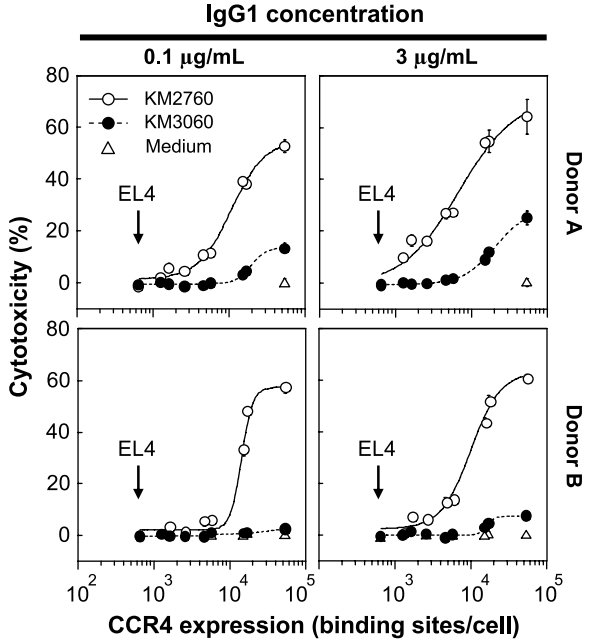

Fig. 3 ADCC of anti-CCR4 IgG1 fucose variants using EL4 transfectant clones with differing antigen expression as target cells. *Y*-axis, cytotoxicities in the presence of anti-CCR4 IgG1s or medium alone determined by 4-hour ^{51}Cr release assays. *X*-axis, number of CCR4 binding sites per cell of each target clone including parent EL4 cells (*arrows*). PBMC from healthy blood donors were used as effector cells, with a constant effector-to target ratio of 25:1. Two different PBMC donors (*donor A* and *donor B*) and IgG1 concentrations (0.1 and 3 μg/mL) were used as indicated.

Natural Killer Cell Binding of IgG1 Fucose Variants. The mechanism responsible for ADCC enhancement by fucose removal from IgG1 is an increase of IgG1 binding to FcγRIIIa (16, 27). This enhancement also results in effective ADCC at a lower antigen density. We have previously shown the improved FcγRIIIa affinity of KM3065 compared with rituximab by ELISA method (31) and determined the kinetic and thermodynamic parameters of the interaction between FcγRIIIa and the two anti-CD20 IgG1s (27). The enhanced FcγRIIIa binding by fucose removal was also confirmed for anti-CCR4 IgG1s (data not shown).

Table 3 Parameters in ADCC plots of anti-CCR4 antibodies

Donor	Antibody	Concentration (μg/mL)	Maximal lysis* (%)	EC_{50} (KM3060†; binding sites)	Ratio
A	KM3060	0.1	13.6	1.98×10^4	×5.6
	KM2760	0.1	55.0	0.36×10^4	
	KM3060	3	28.8	2.13×10^4	×9.6
	KM2760	3	71.8	0.22×10^4	
B	KM3060	0.1	5.66	7.67×10^4	×11
	KM2760	0.1	57.3	0.70×10^4	
	KM3060	3	7.37	1.63×10^4	×9.2
	KM2760	3	63.2	0.18×10^4	

*Estimated by using the four-parameter regression equations.

†Number of CCR4 binding sites per cell required to achieve the half-maximal lysis by KM3060.

Furthermore, the binding of IgG1 fucose variants to purified NK cells prepared from blood of one healthy donor was measured by flow cytometry (Fig. 6). The low-fucose anti-CCR4 and anti-CD20 IgG1s each showed slightly higher binding to NK cells than their highly fucosylated counterparts, which was consistent with the result of other analyses (16). Next, we examined whether IgG1 binding to NK cells was enhanced when anti-CCR4 IgG1 was ligated with clustered antigen (BSA-conjugated CCR4 peptide) to imitate the physiologic condition in which FcγRIIIa molecules on NK cells are cross-linked by the complex of antibody and target cells. Under these conditions, binding to NK cells was further enhanced for each antibody; however, the increase was greater for the low-fucose KM2760.

Antigen-Specific Natural Killer Cell Activation. To investigate whether increased binding of low-fucose IgG1 to FcγRIIIa and NK cells is a key step for NK cell activation during ADCC, we next investigated expression pattern of the activation marker CD69 on $CD56^+$ NK cells in the presence of both anti-CD20 IgG1 and four of the target cell clones with differing CD20 expression levels (EL4, CD20/EL4-C, CD20/EL4-E, and CD20/EL4-G; the numbers of CD20 binding sites per cell of each clone were shown in Table 2). The control experiment was first done by stimulating purified NK cells in the presence of phorbol 12-myristate 13-acetate and ionomycin for 24 hours to confirm the up-regulation of CD69 in whole population of NK cells (Fig. 7*A*).

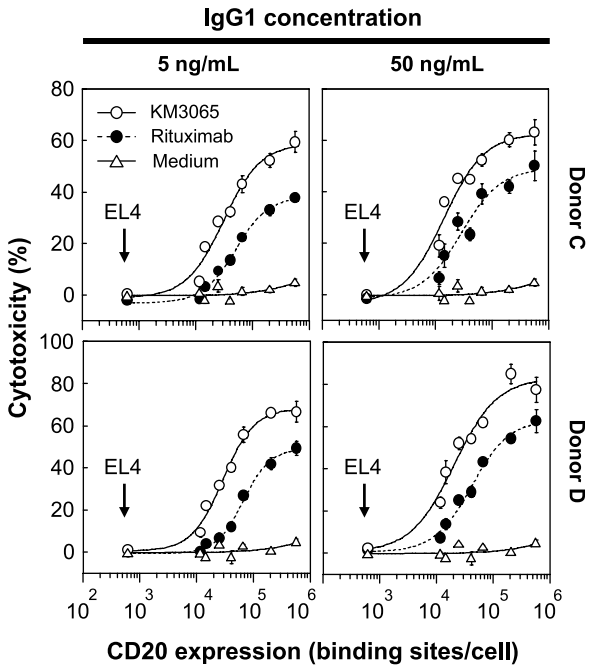

Fig. 4 ADCC of anti-CD20 IgG1 fucose variants using EL4 transfectant clones with differing antigen expression as target cells. *Y*-axis, cytotoxicities in the presence of anti-CD20 IgG1s or medium alone determined by 4-hour ^{51}Cr release assays. *X*-axis, number of CD20 binding sites per cell of each target clones including parent EL4 cells (*arrows*). PBMC from healthy blood donors were used as effector cells, with a constant effector-to target ratios of 25:1. Two different PBMC donors (*donor C* and *donor D*) and IgG1 concentrations (5 and 50 ng/mL) were used as indicated.

Table 4 Parameters in ADCC plots of anti-CD20 antibodies

Donor	Antibody	Concentration (ng/mL)	Maximal lysis* (%)	EC_{50} (rituximab†; binding sites)	Ratio
C	Rituximab	5	38.3	5.62×10^4	×3.0
	KM3065	5	58.8	1.88×10^4	
	Rituximab	50	49.2	2.99×10^4	×2.7
	KM3065	50	62.7	1.10×10^4	
D	Rituximab	5	49.2	6.70×10^4	×3.4
	KM3065	5	68.2	1.99×10^4	
	Rituximab	50	63.3	4.12×10^4	×3.2
	KM3065	50	83.2	1.30×10^4	

*Estimated by using the four-parameter regression equations.
†Number of CD20 binding sites per cell required to achieve the half-maximal lysis by rituximab.

When mixed with the EL4-derived target cells, NK cells could be clearly identified and removed from the flow cytometeric analysis due to their relative small diameter reflected in forward scatter (Fig. 7*B*); accordingly, CD56/CD69 expression levels in NK cells mixed with target cells for 4 and 24 hours were analyzed in the absence or presence of various antibodies (KM3065, rituximab, or anti-CCR4 KM2760 as an irrelevant control antibody; Fig. 7*C*). In the absence of antibody, no CD69 up-regulation was observed either at 4 or 24 hours (Fig. 7*C*, *medium column*), which was consistent with the resistance of the EL4 clones to antibody-independent cytotoxicity observed in the ADCC assays (Figs. 3 and 4).

In the presence of CD20-positive target cells at 4 hours, the two anti-CD20 IgG1s each increased the proportion of activated NK cells in a manner dependent on CD20 expression level. The low-fucose anti-CD20 antibody, KM3065, consistently induced higher numbers of activated NK cells than rituximab: 36% to 45% activation of NK cells for KM3065 versus 8% to 22% for rituximab. At 24 hours, KM3065 activity was increased, but no longer obviously antigen-density dependent, with activation of majority of NK cells (64-71%) irrespective of CD20 expression levels on target cells. With rituximab at 24 hours, the activation was also significantly increased from 4-hour incubation (24-48%), although still lower than that with KM3065, and increased at higher antigen density. NK cell activation by both IgG1s were considered maximal at this time point because the CD69-positive NK cell proportions in the presence of anti-CD20 IgG1s at 24 hours was unchanged when the incubation time was extended to 48 hours (data not shown). Taken together, these results provide evidence of a possible mechanism by which low-fucose IgG1 can increase ADCC on target cells with low antigen expression, namely activation of more NK cells by low fucose antibodies than conventional high-fucose IgG1.

When mixed with CD20-negative EL4 cells and anti-CD20 IgG1, or when mixed with CD20-positive cells and irrelevant IgG1 KM2760, NK cells did not exhibit up-regulated CD69 expression at any time during the experimental period. These results indicate the strict dependency of low-fucose IgG1 in mediating ADCC on the presence of antigen, despite its antigen-independent binding capacity to NK cells as shown in Fig. 6.

There are two distinct subsets of human NK cells identified by cell surface density of CD56: a small population of $CD56^{bright}$ (<10%) and the remainder $CD56^{dim}$ (32). To identify which population was involved in anti-CD20 IgG1-mediated NK cell

activation, the flow cytometer histograms obtained above were reanalyzed according to CD56 expression on NK cells. As a result, no apparent increase in CD69 expression in $CD56^{bright}$ subset was observed in all the samples shown in Fig. 7*C*, suggesting that the NK cell subset responsible for ADCC mediated by both the IgG1 fucose variants was $CD56^{dim}$. An example is shown in Fig. 7*D*, 24-hour incubation in the presence of CD20/EL4-E.

DISCUSSION

One of the major obstacles to optimizing the efficacy of therapeutic antibodies is low and heterogeneous antigen expression that (*a*) allows cells to evade the effective treatment, (*b*) induces the selection of low antigen cell, and (*c*) makes some antigenic targets resistant to antibody therapeutics. For example, the most successful anticancer antibody, rituximab, shows an inferior clinical response rate for lymphoma subtypes that have a relatively lower expression of CD20, such as chronic lymphocytic leukemia or small lymphocytic lymphoma, compared with highly responsive follicular lymphoma with higher CD20 expression, although it should be noted that other factors such as the differential expression of complement-inhibitory proteins (CD46, CD55, CD59) among these clinical subtypes might also affect the rituximab responsiveness (3). It has been shown that antigen expression is a critical factor of the efficacy of the anti-HER2 IgG1 trastuzumab (1, 2, 4, 33), for which treatment is restricted to HER2-overexpressing 20% to 30% breast cancer patients as determined by immunohistochemistry or fluorescence *in situ* hybridization before therapy (34). Trastuzumab-mediated ADCC, considered a critical therapeutic mechanism of the antibody, is dependent on the levels of HER2 on target cells: The antibody can induce ADCC only against tumor cells with $\geq 10^5$ HER2 molecules per cell (35, 36). In addition, residual tumor cells with lower antigen expression could escape from antibody therapy, which might lead to relapse and resultant poor prognosis. As the problem of the low or heterogeneous antigen expression on target cells is relevant for many other therapeutic antibodies, enhanced ADCC due to the augmentation of low-fucose IgG1 binding to FcγRIIIa is a promising way to address this problem.

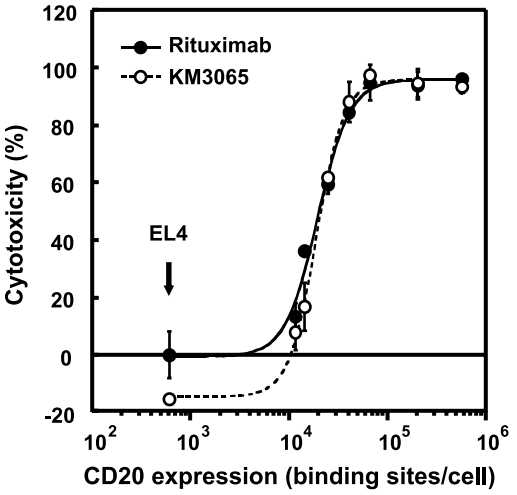

Fig. 5 CDC of anti CD20 IgG1 fucose variants against clones with differing CD20 expression as the target cell. IgG1 concentration used was 1 μg/mL. CDC against parent EL4 cells is also shown (*arrow*).

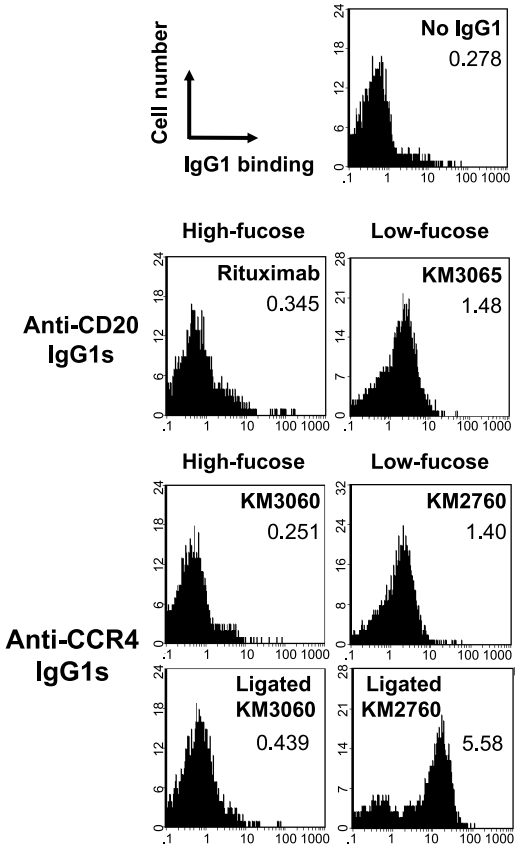

Fig. 6 NK cell binding of IgG1 fucose variants by flow cytometry. Antibodies used to stain NK cells and mean fluorescence intensity values are indicated. In some experiments, anti-CCR4 IgG1s were ligated with BSA-conjugated CCR4 peptide (20 μg/mL) by the 10-minute preincubation of IgG1s and the conjugate on ice. Data are representative of two repeat experiments.

Previous studies have only shown the enhanced ADCC of low-fucose IgG1 upon target cell lines with a fixed and relatively high density of antigen (16–18). How the antigen expression of target cells modulates the advantage by fucose reduction on ADCC remained unanswered. To investigate whether low-fucose IgG1 could exhibit potent ADCC on target cells with less antigen amount, we constructed panels of target cells with a range of known antigen expression levels. Because the obtained clones were uniform in their cell diameters and susceptibilities to antigen-independent lysis by NK cells, the use of these experimental target cells enabled the measurement of the dependence of ADCC activity on antigen amount, and hence density, per target cell. Interestingly, antigen amount required for ADCC induction for low-fucose IgG1 was lower than that for high-fucose IgG1, suggesting that improvement of IgG1 binding to FcγRIIIa on effector cells by fucose depletion can reduce antigen amount necessary for ADCC induction. Because the antigen-binding activities do not vary among fucose variant IgG1s and consequently the IgG1 amount bound on the surface

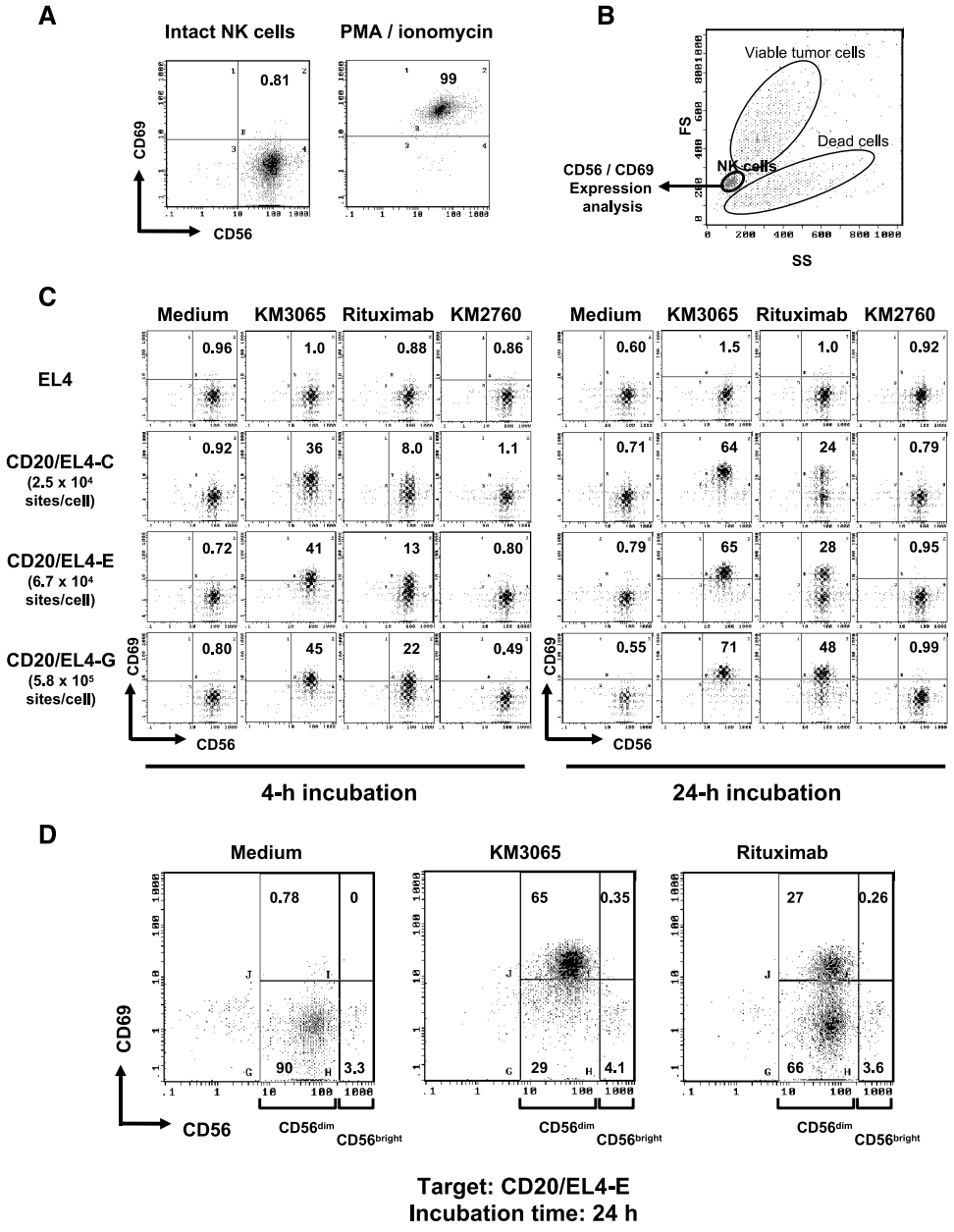

Fig. 7 NK cell activation during ADCC analyzed by flow cytometry. Figures show the proportion (%) of $CD56^+CD69^+$ cells. *A,* NK cells purified from PBMC using MACS displayed $CD56^+CD69$ and phenotype (*left*). After control stimulation in the presence of phorbol 12-myristate 13-acetate and ionomycin for 24 hours, 99% of the cells had up-regulated surface CD69 expression. *C,* analysis of CD69 expression on NK cells in the presence of target cells and antibodies. One hundred thousand NK cells and an equal number of the indicated target cells were mixed in a round-bottomed 96-well plate in the presence of the indicated IgG1 at the final concentration of 1 μg/mL or medium alone. After incubation for 4 hours (*left*) or 24 hours (*right*), cells were harvested and subjected to CD69/CD56 expression analysis. The cytograms are the CD69/CD56 expression of NK cells gated out from the whole cell mixture by their relatively small forward scatter/side scatter value (*B*). Figures show the percentage of $CD56^+CD69^+$ cells. *D,* an example of the reanalysis of NK cells according to their CD56 density. $CD56^+$ compartment was further divided into $CD56^{dim}$ and $CD56^{bright}$ populations. Figures show the percentage of the cell in each analyzed compartment.

of target cells were unaffected by fucose content in IgG1 as confirmed by flow cytometry (data not shown), the potent ADCC induction by low-fucose IgG1 might be due to the efficient activation of effector cells via more effective interactions with FcγRIIIa even in the presence of low IgG1 density on target cells.

Although we did not investigate *FCGR3A*-158 genotype of the PBMC donors in the current studies, *FCGR3A*-158V/F polymorphism is also likely to affect the antigen density required for ADCC because our data imply that IgG1-FcγRIIIa affinity affects the antigen density threshold required for ADCC induction. However, fucose depletion is expected to lower the required antigen density for any PBMC donors because it improves IgG1-FcγRIIIa binding independently of the *FCGR3A* genotypes (31), although the difference in required antigen

densities between IgG1 fucose variants may vary with the *FCGR3A* genotype.

Although reduction of fucose showed the benefits of ADCC induction in low antigen density for both CCR4 and CD20 specificities, the CCR4 system displayed a more marked difference between ADCC of fucose variants than CD20 system. Possible explanations for this difference include the following: The higher amount of CD20 on the experimental target cells (approximately one order of magnitude higher than CCR4; Table 2) might be enough for the ADCC induction of high-fucose IgG1. Alternatively, the inherent structures of each antigen molecules, especially the mobility and the configuration of the molecules in lipid bilayer on cell surface, might affect the efficacy of high-fucose IgG1. In contrast to CCR4, which is a seven-transmembrane-spanning G-coupled receptor (37) and is presumed to have poor mobility in lipid bilayer, CD20 is highly mobile and naturally forms multimer (38–40). In addition, most of anti-CD20 antibodies including rituximab can redistribute CD20 into lipid rafts, which determines the capacity to induce strong CDC (41). Although the relation of ADCC and the redistribution into lipid rafts has been poorly defined, high density of IgG1 bound on CD20 multimer or localized CD20 in lipid rafts may induce ADCC even by high-fucose IgG1. The hypothesis that clustering IgG1 could enhance ADCC is supported by the reports of dimerized antibodies having potent ADCC (42, 43).

As expected from the identical binding capacities of fucose variant IgG1s to C1q (16), KM3065 and rituximab did not vary in their CDC activities against the target cell clones with varying antigen expression. Although the anti-CD20 IgG1s exerted CDC even upon low or intermediate $CD20^+$ clones, whose antigen expression levels overlapped with those of higher CCR4 expressing clones, anti-CCR4 IgG1s did not mediate detectable CDC activity against all $CCR4^+$ clones. This discrepancy may again support the hypothesis that CCR4 and CD20 might differ in their inherent properties of the molecule, such as clustering capacity in lipid bilayer, which is critical for CDC susceptibility (41) and possibly affect the susceptibility to high-fucose IgG1-mediated ADCC shown in Fig. 4. Because the low-fucose anti-CCR4 IgG1 greatly augmented the ADCC of high-fucose anti-CCR4 IgG1, the inability of anti-CCR4 antibody to mediate CDC also implies the therapeutic benefit of low-fucose IgG1 that it would be applicable for wider range of molecular targets where CDC cannot be expected due to inherent molecular properties of the antigen.

We further investigated the mechanism of enhanced ADCC by low-fucose IgG1 in terms of NK cell activation. Consistent with the ADCC analysis, KM3065 induced more CD69-positive activated NK cells than rituximab even in the presence of lower antigen density, suggesting that low-fucose IgG1 can efficiently recruit and activate effector cells via the increased binding to FcγRIIIa. The activated NK subset was predominantly $CD56^{dim}$, a not unexpected finding because $CD56^{bright}$ NK cells express low level of FcγRIIIa and are presumed to function as cytokine responder/producer cells rather than cytotoxic killer cells (30, 44–46). Further, NK cells were shown to be activated only by IgG1 bound on target cells despite low-fucose IgG1 itself could bind slightly to NK cells in the absence of antigen (Fig. 6). This is a very important finding as it suggests that enhanced FcγRIIIa/NK interactions should not induce nonspecific side effects. The mechanism of the tumor-specific activation of NK cells via low-fucose IgG1 remains unknown; however, it may be that intracellular signals through FcγRIIIa are not triggered until the density of receptor-bound IgG1 is elevated above a minimal level by antigen molecules present on target cells. Enhanced binding of low-fucose IgG1 to FcγRIIIa might lower the threshold of IgG1 density on target cells necessary for NK cell activation and consequently results in ADCC induction against targets with fewer antigen molecules. This hypothesis is supported by the results herein that low-fucose IgG1 binding was greatly enhanced by preligating the antibody with antigen to mimic cell-surface antigen-antibody clusters increase NK cell binding at concentration of highly fucosylated IgG1 did not bind (Fig. 6).

In conclusion, our data showed that low-fucose IgG1 shows potent ADCC upon target cells with lower antigen density compared with conventional antibodies, through the effective and antigen-specific activation of NK cells due to augmented binding to FcγRIIIa. These features of low-fucose IgG1 could be therapeutically beneficial because clinical tumors often display the heterogeneity in their antigen expression levels and in addition the number of effector cells accessible to *in vivo* tumor would be fewer compared with *in vitro* experimental condition.

ACKNOWLEDGMENTS

We thank Dr. Philip Wallace for helpful suggestions and critical reading of the manuscript.

REFERENCES

1. Carter P. Improving the efficacy of antibody-based cancer therapies. Nat Rev Cancer 2001;1:118–29.

2. Glennie MJ, van de Winkel JGJ. Renaissance of cancer therapeutic antibodies. Drug Discov Today 2003;8:503–10.

3. Smith MR. Rituximab (monoclonal anti-CD20 antibody): mechanisms of action and resistance. Oncogene 2003;22:7359–68.

4. Clynes RA, Towers TL, Presta LG, Ravetch JV. Inhibitory Fc receptors modulate *in vivo* cytoxicity against tumor targets. Nat Med 2000;6:443–6.

5. Cartron G, Dacheux L, Salles G, et al. Therapeutic activity of humanized anti-CD20 monoclonal antibody and polymorphism in IgG Fc receptor FcγRIIIa gene. Blood 2002;99:754–8.

6. Anolik JH, Campbell D, Felgar RE, et al. The relationship of FcγRIIIa genotype to degree of B cell depletion by rituximab in the treatment of systemic lupus erythematosus. Arthritis Rheum 2003;48:455–9.

7. Weng WK, Levy R. Two immunoglobulin G fragment C receptor polymorphisms independently predict response to rituximab in patients with follicular lymphoma. J Clin Oncol 2003;21:3940–7.

8. Koene HR, Kleijer M, Algra J, von Roos D, dem Born AE, de Haas M. FcγRIIIa-158V/F polymorphism influences the binding of IgG by natural killer cell FcγRIIIa, independently of the FcγRIIIa-48L/R/H phenotype. Blood 1997;90:1109–14.

9. Wu J, Edberg JC, Redecha PB, et al. A novel polymorphism of FcγRIIIa (CD16) alters receptor function and predisposes to autoimmune disease. J Clin Invest 1997;100:1059–70.

10. Leget GA, Czuczman MS. Use of rituximab, the new FDA-approved antibody. Curr Opin Oncol 1998;10:548–51.

11. Gopal AK, Press OW. Clinical applications of anti-CD20 antibodies. J Lab Clin Med 1999;134:445–50.

12. Kumpel BM, Rademacher TW, Rook GA, Williams PJ, Wilson IB. Galactosylation of human IgG monoclonal anti-D produced by EBV-transformed B lymphoblastoid cell lines is dependent on culture method and affects Fc receptor-mediated functional activity. Hum Antib Hybrid 1994;5:143–51.

13. Kumpel BM, Wang Y, Griffiths HL, Hadley AG, Rook GA. The biological activity of human monoclonal IgG anti-D is reduced by β-galactosidase treatment. Hum Antib Hybrid 1995;6: 82–8.

14. Umana P, Jean-Mairet J, Moudry R, Amstutz H, Bailey JE. Engineered glycoforms of an antineuroblastoma IgG1 with optimized antibody-dependent cellular cytotoxic activity. Nat Biotechnol 1999;17: 176–80.

15. Davies J, Jiang L, Pan LZ, LaBarre MJ, Anderson D, Reff M. Expression of GnTIII in a recombinant anti-CD20 CHO production cell line: expression of antibodies with altered glycoforms leads to an increase in ADCC through higher affinity for FcγRIII. Biotechnol Bioeng 2001;74:288–94.

16. Shields RL, Lai J, Keck R. Lack of fucose on human IgG1 N-linked oligosaccharide improves binding to human FcγRIII and antibody-dependent cellular toxicity. J Biol Chem 2002;277: 26733–40.

17. Shinkawa T, Nakamura K, Yamane N, et al. The absence of fucose but not the presence of galactose or bisecting *N*-acetylglucosamine of human IgG1 complex-type oligosaccharides shows the critical role of enhancing antibody-dependent cellular cytotoxicity. J Biol Chem 2003;278:3466–73.

18. Niwa R, Shoji-Hosaka E, Sakurada M, et al. Defucosylated anti-CC chemokine receptor 4 IgG1 with enhanced antibody-dependent cellular cytotoxicity shows potent therapeutic activity to T cell leukemia and lymphoma. Cancer Res 2004:64:2127–33.

19. Yamane-Ohnuki N, Kinoshita S, Inoue-Urakubo M, et al. Establishment of FUT8 knock-out CHO cells; an ideal host cell line for producing completely defucosylated antibodies with enhanced ADCC. Biotechnol Bioeng 2004;87:614–22.

20. Ross JS, Fletcher JA. The HER-2/neu oncogene in breast cancer: prognostic factor, predictive factor, and target for therapy. Stem Cells 1998;16:413–28.

21. Davis TA, Czerwinski DK, Levy R. Therapy of B-cell lymphoma with anti-CD20 antibodies can result in the loss of CD20 antigen expression. Clin Cancer Res 1999;5:611–5.

22. Kennedy AD, Beum PV, Solga MD, et al. Rituximab infusion promotes rapid complement depletion and acute CD20 loss in chronic lymphocytic leukemia. J Immunol 2004;172:3280–8.

23. Lustig HJ, Bianco C. Antibody-mediated cell cytotoxicity in a defined system: regulation by antigen, antibody, and complement. J Immunol 1976;116:253–60.

24. Nakamura K, Tanaka Y, Fujino I, Hirayama N, Shitara K, Hanai N. Dissection and optimization of immune effector functions of humanized anti-ganglioside GM2 monoclonal antibody. Mol Immunol 2000;37: 1035–46.

25. Brockhoff G, Hoftstaedter F, Knuechel R. Flow cytometric detection and quantitation of the epidermal growth factor receptor in comparison to Scatchard analysis in human bladder carcinoma cell lines. Cytometry 1994;17:75–83.

26. Peeters JM, Hazendonk TG, Beuvery EC, Tesser GI. Comparison of four bifunctional reagents for coupling peptides to proteins and the effect of the three moieties on the immunogenicity of the conjugates. J Immunol Meth 1989;120:133–43.

27. Okazaki A, Shoji-Hosaka E, Nakamura K, et al. Fucose depletion from human IgG1 oligosaccharide enhances binding enthalpy and association rate between IgG1 and FcγRIIIa. J Mol Biol 2004;336: 1239–49.

28. Vervoordeldonk SF, Merle PA, van Leeuwen EF, von dem Borne AE, Slaper-Cortenbach IC. Preclinical studies with radiolabeled monoclonal antibodies for treatment of patients with B-cell malignancies. Cancer 1994;73:1006–11.

29. Ginardi L, De Martinis M, Matutes E, Farahat N, Morilla R, Catovsky D. Levels of expression of CD19 and CD20 in chronic B cell leukaemias. J Clin Pathol 1998;51:364–69.

30. Bellosillo B, Villamor N, Lopez-Guillermo A, et al. Complement-mediated cell death induced by rituximab in B-cell lymphoproliferative disorders is mediated *in vitro* by a caspase-independent mechanism involving the generation of reactive oxygen species. Blood 2001;98: 2771–7.

31. Niwa R, Hatanaka S, Shoji-Hosaka E, et al. Enhancement of the antibody-dependent cellular cytotoxicity of low-fucose IgG1 is independent of FcγRIIIa functional polymorphism. Clin Cancer Res 2004;10: 6248–55.

32. Lanier LL, Le AM, Civin CI, Loken MR, Phillips JH. The relationship of CD16 (Leu-11) and Leu-19 (NKH-1) antigen expression on human peripheral blood NK cells and cytotoxic T lymphocytes. J Immunol 1986;136:4480–6.

33. Carter P, Presta L, Gorman CM, et al. Humanization of an anti-p185HER2 antibody for human cancer therapy. Proc Natl Acad Sci U S A 1992;89:4285–9.

34. Pauletti G, Dandekar S, Rong H, et al. Assessment of methods for tissue-based detection of the HER-2/neu alteration in human breast cancer: a direct comparison of fluorescence *in situ* hybridization and immunohistochemistry. J Clin Oncol 2000;18:3651–64.

35. Lewis GD, Figari I, Fendly B, et al. Differential responses of human tumor cell lines to anti-p185HER2 monoclonal antibodies. Cancer Immunol Immunother 1993;37:255–63.

36. Sarup JC, Johnson RM, King KL, et al. Characterization of an anti-p185HER2 monoclonal antibody that stimulates receptor function and inhibits tumor cell growth. Growth Regulation 1991;1:72–82.

37. Power CA, Meyer A, Nemeth K, et al. Molecular cloning and functional expression of a novel CC chemokine receptor cDNA from a human basophilic cell line. J Biol Chem 1995;270:19495–500.

38. Deans JP, Robbins SM, Polyak MJ, Savage JA. Rapid redistribution of CD20 to a low density detergent-insoluble membrane compartment. J Biol Chem 1998;273:344–8.

39. Polyak MJ, Tailor SH, Deans JP. Identification of a cytoplasmic region of CD20 required for its redistribution to a detergent-insoluble membrane compartment. J Immunol 1998;161:3242–8.

40. Bubien JK, Zhou LJ, Bell PD, Frizzell RA, Tedder TF. Transfection of the CD20 cell surface molecule into ectopic cell types generates a Ca^{2+} conductance found constitutively in B lymphocytes. J Cell Biol 1993;121:1121–32.

41. Cragg MS, Morgan SM, Chan HT, et al. Complement-mediated lysis by anti-CD20 mAb correlates with segregation into lipid rafts. Blood 2003;101:1045–52.

42. Caron PC, Laird W, Co MS, Avdalovic NM, Queen C, Scheinberg DA. Engineered humanized dimeric forms of IgG are more effective antibodies. J Exp Med 1992;176:1191–5.

43. Nielsen SU, Routledge EG. Human T cells resistant to complement lysis by bivalent antibody can be efficiently lysed by dimers of monovalent antibody. Blood 2002;100:4067–73.

44. Caligiuri MA, Zmuidzinas A, Manley TJ, Levine H, Smith KA, Ritz J. Functional consequences of interleukin 2 receptor expression on resting human lymphocytes. Identification of a novel natural killer cell subset with high affinity receptors. J Exp Med 1990;171: 1509–26.

45. Baume DM, Robertson MJ, Levine H, Manley TJ, Schow PW, Ritz J. Differential responses to interleukin 2 define functionally distinct subsets of human natural killer cells. Eur J Immunol 1992;22:1–6.

46. Nagler A, Lanier LL, Cwirla S, Phillips JH. Comparative studies of human FcRIII-positive and negative natural killer cells. J Immunol 1989; 143:3183–91.